J|A|C|S
ARTICLES
Published on Web 01/25/2006

Electrochemistry of Immobilized Redox Enzymes: Kinetic Characteristics of NADH Oxidation Catalysis at Diaphorase Monolayers Affinity Immobilized on Electrodes.

Benoît Limoges,* Damien Marchal, François Mavré, and Jean-Michel Savéant*

Contribution from the Laboratoire d'Electrochimie Moléculaire, Université de Paris 7-Denis Diderot, 2 place Jussieu,75251 Paris Cedex 05, France

Received October 10, 2005; E-mail: saveant@paris7.jussieu.fr; limoges@paris7.jussieu.fr

Abstract: In the class of NADH:acceptor oxidoreductases, the diaphorase from *Bacillus stearothermophilus* is a particularly promising enzyme for sensing NADH, and indirectly a great number of analytes, when coupled with a NAD-dependent dehydrogenase as well as for the design of mono- and multienzyme affinity sensors. The design and rational optimization of such systems require devising immobilization procedures that prevent dramatic losses of the enzymatic activity and a full kinetic characterization of the immobilized enzyme system. Two immobilization procedures are described, which involve recognition of the biotinylated diaphorase by a monolayer of neutravidin adsorbed on the electrode surface either directly or through the intermediacy of a monolayer of biotinylated rabbit immunoglobulin. Thorough kinetic characterization of the two systems is derived from cyclic voltammetric responses. A precise estimate of the enzyme coverages is obtained after comparing the enzyme kinetics of the immobilized and the homogeneous system.

Introduction

The main applications of electrochemical enzymatic catalysis with enzymes immobilized on the electrode surface encompass two broad domains. One involves sensing the enzyme substrate. The simplest systems use a redox enzyme, with electron transfer between the electrode and the enzyme being either direct or by means of a mediator that serves as a cosubstrate to the enzyme.[1] Coupling several enzymes through their substrates and products, which need not be redox enzymes with the exception of the last one in the cascade, can considerably enlarge the scope of these systems in terms of analyzable substrates.[2] A second type of applications relates to affinity biosensing (as, for example, in electrochemical immuno- and DNA-sensors). One of the two complementary molecules is immobilized on the electrode surface, while the other member of the couple stands in the solution after being labeled by a redox active molecule.[3] In this framework, enzyme labeling is a powerful manner of amplifying the electrochemical response compared to simple redox labels.[4] Coupling of several enzymes in this case is a promising way of boosting amplification.[5] The rational development of reproducible and sensitive systems in these two areas requires progressing in two directions. One deals with the design and testing of gentle immobilization procedures that prevent dramatic losses of the enzymatic activity, as often happens with chemical methods. The second involves the development and effective use of theoretical tools required for relating the electrochemical responses to the mechanism and kinetic characteristics of the enzymatic reaction in the framework of an electrochemical technique.

Diaphorases, and more specifically the diaphorase from *Bacillus stearothermophilus* (DI), provide a good illustration of the above-mentioned problems. Potentially, DI is a particularly promising enzyme because of a series of favorable features. It is a NADH:acceptor oxidoreductase with a flavin mononucleotide (FMN) prosthetic group[6] that catalyses the hydride or electrons transfer from NADH to a variety of hydride or electron acceptors.[6,7] Its remarkable thermal stability (up to 70 °C), insensitivity to dioxygen, and the high rates of its reaction with NADH make it a good candidate for the above-mentioned applications. Regarding the detection of NADH, one thus expects minimizing interferences of easily oxidizable species such as ascorbate, urate, and acetaminophen that might be present in biological samples. Immobilized diaphorase electrodes are also expected to have a better reactivity and specificity than electrocatalytic methods based on the oxidation of NADH by organic or inorganic redox catalysts attached to the electrode surface.[8] Another potential advantage derives from the fact that

(1) (a) Armstrong, F. A.; Wilson, G. S. *Electrochim. Acta* **2000**, *45*, 2623. (b) Wilson, G. S.; Hu, Y. *Chem. Rev.* **2000**, *100*, 2693. (c) Ikeda, T. *Bull. Electrochem.* **1992**, *8*, 145. (d) Campbell, C. N.; Heller, A.; Caruana, D. J.; Schmidtke, D. W. In *Electroanalytical Methods for Biological Materials*; Brajter-Toth, A., Chambers, J. Q., Eds.; Marcel Dekker: New York, 2002.
(2) (a) Willner, I.; Katz, E. *Angew. Chem., Int. Ed*. **2000**, *39*, 1180. (b) Gorton, L. *Electroanalysis* **1995**, *7*, 23.
(3) (a) Warsinke, A.; Benkert, A.; Scheller, F. W. *Fresenius' J. Anal. Chem.* **2000**, *366*, 622. (b) Wang, J. *Chem.*−*Eur. J.* **1999**, *5*, 1681. (c) Skladal, P. *Electroanalysis* **1997**, *9*, 737.
(4) (a) Azek, F.; Grossiord, C.; Joannes, M.; Limoges, B.; Brossier, P. *Anal. Biochem.* **2000**, *284*, 107. (b) Caruana, D. J.; Heller A. *J. Am. Chem. Soc.* **1999**, *121*, 769. (c) Gyss, C.; Bourdillon, C. *Anal. Chem.* **1987**, *59*, 2350.
(5) (a) Scheller, F. W.; Bauer, C. G.; Makower, A.; Wollenberger, U.; Warsinke, A.; Bier, F. F. *Anal. Lett.* **2001**, *34*, 1233. (b) Bauer, C. G.; Eremenko, A. V.; Ehrentreich-Förster, E.; Bier, F. F.; Makower, A.; Halsall, H. B.; Heineman, W. R.; Scheller, F. W. *Anal. Chem.* **1996**, *68*, 2453.
(6) Matsue, T.; Yamada, H.; Chang, H.-C.; Uchida, I.; Nagata, K.; Tomoita, K. *Biochim. Biophys. Acta* **1990**, *1038*, 29.
(7) Ogino, Y.; Takagi, K.; Kano, K.; Ikeda, T. *J. Electroanal. Chem.* **1995**, *396*, 517.
(8) Gorton, L.; Dominguez, E. *Rev. Mol. Biotechnol.* **2002**, *82*, 371.

10.1021/ja0569196 CCC: $33.50

the NADH/NAD^+ couple is the cofactor of several hundreds of dehydrogenase enzymes. Mediated electro-oxidation of NADH to enzymatically active NAD^+ via diaphorase therefore offers a possibility to detect the substrates of these enzymes, thus opening a route to the determination of a large number of biological molecules of analytical interest in clinical and food chemistry.

Monoenzymatic[9−12] and bienzymatic[13−18] diaphorase-immobilized systems have accordingly been proposed to exploit these possibilities. However, due to the lack of appropriate theoretical tools at the time, the kinetics and mechanisms could not be reliably analyzed, hampering the optimization of the analytical methods proposed. This is particularly important for the design and testing of bienzymatic systems for the applications just mentioned and also for affinity biosensing applications. In the latter case, bienzymatic amplification has been extensively applied to spectrophotometric immunoassays[19] but very rarely to electrochemical immunoassays.[20]

Although the previous estimations of the amount of active enzyme immobilized were approximate, it appears that the immobilization procedure, based on the use of glutaraldehyde as cross-linking reagent,[9,10,21] leads to the inactivation of a large fraction of the enzyme.[9b,10] An additional drawback of the procedures used is that they require large amounts of enzyme in the coupling solution (enzyme concentrations as large as 0.1 mM[9a,10] or even 1 mM[9b,c,21]), which may cause nonspecific aggregation of the enzyme leading to the formation of ill-defined and poorly stable enzyme layers on the electrode surface.

The work reported below consequently addressed two problems. One is the design of procedures that lead to a stable and well-defined deposition of the enzyme, minimizing the loss of its catalytic function through partial denaturation, steric hindrance, and/or conformational changes. In this purpose, we resorted to a bioaffinity-based immobilization procedure. Submicromolar concentrations of enzyme are then usually sufficient to saturate a solid surface with an enzyme monolayer.[22] With such procedures, we expect to fully preserve the catalytic activity of the enzyme, as was previously demonstrated with glucose oxidase attached to the electrode by means of antigen−antibody interactions,[23] with horseradish peroxidase immobilized by way of an avidin−biotin linkage,[24] or with a ferredoxin $NADP^+$ reductase immobilized through metal-chelating ligand self-assembled on a gold electrode.[25]

Our second objective is to analyze thoroughly, by means of cyclic voltammetry, the enzymatic kinetics of the reactions that take place at these electrodes. On the basis of the theory available for ping-pong mechanisms and immobilized enzymes, it is indeed possible to relate the voltammetric responses to the characteristic rate constants, the substrate and cosubstrate concentrations, the mass transport parameters and the enzyme surface coverage.[26] A complete analysis requires that the kinetic characteristics of the immobilized enzyme be compared with their homogeneous counterparts. Although the previous analyses in this area[7,27] could use existing theoretical treatments, these were limited to first-order conditions.[28] In fact, owing to the very high values attained by the bimolecular rate constant between DI and many cosubstrates ($>10^8$ M^{-1} s^{-1}), the pseudo-first-order approximation is only valid at very low mediator concentrations ($<10^{-7}$ M). As to the kinetic parameters of the reductive half-reaction with NADH, the particular conditions used to preserve the steady-state response at low substrate concentrations (i.e., enzymatic regeneration of NADH from NAD^+ by a lactate dehydrogenase to compensate substrate depletion near the electrode surface) led to a significant underestimation of the substrate kinetic rate constants.[27] The resulting uncertainties in the values of the characteristic rate constants of DI necessitated a thorough reexamination of the homogeneous kinetics of the two half-reactions as a prelude to our main objective, the characterization of the immobilized enzyme systems.

Results and Discussion

Mechanisms, Rate Equation, and Definition of the Pertinent Rate Constants. As cosubstrates, we used one-electron acceptors (transition-metal complexes) as well as two-electron two-proton acceptors (quinones). In the first case, the reaction of the flavin mononucleotide (FMN) prosthetic group with the one-electron acceptor, noted Q, involves the sequence shown in Scheme 1. The first step of the oxidative half-reaction involves $FMNH^-$ rather than $FMNH_2$, both because at the optimal enzymatic pH of 8.5, where we operate, it predominates at equilibrium (the free $FMNH_2/FMNH^-$ couple has a pK_a of 6.7[29]) and because it is easier to oxidize. The electron acceptor Q, generated at the electrode from P by a one-electron transfer, is assumed to react according to a Michaelis−Menten scheme involving a set of three rate constants, $k_{2,1}$, $k_{2,-1}$, $k_{2,2}$, as defined in Scheme 1. The neutral radical form, $FMNH^{\bullet}$, is then oxidized according to a one-electron one-proton global exchange process to finally produce the FMN form. This reaction may follow

(9) (a) Sawaguchi, T.; Matsue, T.; Uchida, I. *Bioelectrochem. Bioenerg.* **1992**, *29*, 127. (b) Yamada, H.; Shiku, H.; Matsue, T.; Uchida, I. *Bioelectrochem. Bioenerg.* **1993**, *29*, 337. (c) Chang, H.-S.; Ueno, A.; Yamada, H.; Matsue, T.; Uchida, I. *Analyst* **1991**, *116*, 793.
(10) Sato, A.; Kano, K.; Ikeda, T. *Chem. Lett.* **2003**, *32*, 880.
(11) Tatsuma, T.; Watanabe, T. *J. Electroanal. Chem.* **1991**, *310*, 149.
(12) Antiochia, R.; Cass, A. E. G.; Palleschi, G. *Anal. Chim. Acta* **1997**, *345*, 17.
(13) Tang, X.; Johansson, G. *Anal. Lett.* **1995**, *28*, 2595.
(14) Gros, P.; Comtat, M. *Biosens. Bioelectron.* **2004**, *20*, 204.
(15) Maines, A.; Prodromidis, M. I.; Tzouwara-Karayanni, S. M.; Karayannis, M. I.; Ashworth, D.; Vadgama, P. *Anal. Chim. Acta* **2000**, 408, 217.
(16) Kashiwagi, Y.; Pan, Q.; Kurashima, F.; Kikuchi, C.; Anzai, J.-I.; Osa, T. *Chem. Lett.* **1998**, *2*, 143.
(17) Montagne, M.; Erdmann, H.; Comtat, M.; Marty, J.-L. *Sens. Actuators, B* **1995**, *27*, 440.
(18) Treloar, P. H.; Christie, I. M.; Kane, J. W.; Crump, P.; Nkohkwo, A. T.; Vadgama, P. M. *Electroanalysis* **1995**, 7, 216.
(19) (a) Loevgren, U.; Kronkvist, K.; Johansson, G.; Edholm, L.-E. *Anal. Chim. Acta* **1994**, *288*, 227. (b) Johannsson, A.; Ellis, D. H.; Bates, D. L.; Plumb, A. M.; Stanley, C. J. *J. Immunol. Methods* **1986**, *87*, 7. (c) Ishizuka, T.; Kawagoe, M.; Suzuki, K.; Hara, M.; Harigai, M.; Kawakami, M.; Kawaguchi, Y.; Hidaka, T.; Matsuki, Y.; Tanaka, N.; Kitani, A.; Nakamura, H. *J. Immunol. Methods* **1992**, *30*, 213. (d) Lövgrena, U.; Kronkvist, K.; Johansson, G.; Edholm, L.-E. *Anal. Chim. Acta* **1994**, *288*, 227. (e) These studies used diaphorases that are much less efficient than the diaphorase from *Bacillus stearothermophilus*. The latter is henceforth commercially available for this purpose.
(20) Cardosi, M. F.; Birch, S. W.; Stanley, C. J.; Johannsson, A.; Turner, A. P. F. *Am. Biotechnol. Lab.* **1989**, *7*, 50.
(21) (a) Yamada, H.; Shiku, H.; Matsue, T.; Uchida, I. *Bioelectrochem. Bioenerg.* **1994**, *33*, 91. (b) Yamada, H.; Fukumoto, H.; Yokoyama, T.; Koike, T. *Anal. Chem.* **2005**, *77*, 1785. (c) Shiku, H.; Takeda, T.; Yamada, H.; Matsue, H. T.; Uchida, I. *Anal. Chem.* **1995**, *67*, 312.
(22) Saleemuddin, M. *Adv. Biochem. Eng. Biotechnol.* **1999**, *64*, 203.
(23) Bourdillon, C.; Demaille, C.; Gueris, C.; Moiroux, J.; Savéant, J.-M. *J. Am. Chem. Soc.* **1993**, *115*, 12264.
(24) Limoges, B.; Yazidi, D.; Savéant, J.-M. *J. Am. Chem. Soc.* **2003**, *125*, 9122.
(25) Madoz-Gúrpide, J.; Abad, J. M.; Fernández-Recio, J.; Vélez, M.; Vázquez, L.; Gómez-Moreno, C.; Fernández, V. M. *J. Am. Chem. Soc.* **2000**, *122*, 9808.
(26) Limoges, B.; Moiroux, J.; Savéant, J.-M. *J. Electroanal. Chem.* **2002**, *521*, 8.
(27) Takagi, K.; Kano, K.; Ikeda, T. *J. Electroanal. Chem.* **1998**, *445*, 211.
(28) (a) Savéant, J.-M.; Vianello, E. In *Advances in Polarography*; Longmuir, I. S., Ed.; Pergamon Press: London, 1960; Vol. 1, pp 367−374. (b) Savéant, J.-M.; Vianello, E. *Electrochim Acta* **1965**, *10*, 905.
(29) Mayhew, S. G. *Eur. J. Biochem.* **1999**, *265*, 698.

Scheme 1

$$NADH + E_{FMN} \underset{k_{1,-1}}{\overset{k_{1,1}}{\rightleftharpoons}} E_{(FMN,NADH)} \xrightarrow{k_{1,2}} NAD^+ + E_{FMNH^-} \quad [1]$$

One-electron acceptors:

$$P \rightleftharpoons Q + e^-$$

$$Q + E_{FMNH^-} \underset{k_{2',-1}}{\overset{k_{2',1}}{\rightleftharpoons}} E_{(FMNH^-,Q)} \xrightarrow{k_{2',2}} P + E_{FMNH^\bullet} \quad [2']$$

$$E_{FMNH^\bullet} \rightleftharpoons E_{FMN^{\bullet -}} + H^+ \qquad K_3$$

$$Q + E_{FMN^{\bullet -}} \underset{k_{3',-1}}{\overset{k_{3',1}}{\rightleftharpoons}} E_{(FMN^{\bullet -},Q)} \xrightarrow{k_{3',2}} P + E_{FMN} \quad [3']$$

Two-electron acceptors:

$$P \rightleftharpoons Q + 2e^-$$

$$Q + E_{FMNH^-} \underset{k_{2,-1}}{\overset{k_{2,1}}{\rightleftharpoons}} E_{(FMNH^-,Q)} \xrightarrow{k_{2,2}} P + E_{FMN} \quad [2]$$

two concurrent pathways. The one shown in Scheme 1 involves an initial deprotonation step, yielding the anion radical form $FMN^{\bullet -}$, which is then oxidized by another Q molecule. The other pathway, conversely (not shown in Scheme 1), involves first the oxidation of the $FMNH^\bullet$ form, yielding the cationic form $FMNH^+$, followed by deprotonation. The $FMNH^\bullet$ form is likely to be more acidic than the $FMNH_2$ form. Therefore, at a pH of 8.5, the first pathway is likely to predominate over the second.

The reductive half-reaction is written in Scheme 1 as a two-step Michaelis−Menten type reaction involving the specific reversible binding of a transient precursor complex followed by a hydride transfer process rather than a $e^- + H^+ + e^-$ reaction sequence, in line with what is generally assumed for enzymes[30] and model systems.[31]

In all cases, the rate at which Q is consumed at steady state is related to the various concentrations and rate constants by eq 1 in the homogeneous and immobilized cases, respectively.[32]

$$\frac{2C_E^0(\text{or } \Gamma_E^0)}{rate} = \frac{1}{k_{1,2}} + \frac{1}{k_{2',2}} + \frac{1}{k_{3',2}} + \frac{1}{k_1[S]_{x=0}} + \frac{1}{k_{2'}[Q]_{x=0}} + \frac{1}{k_{3'}[Q]_{x=0}} \quad (1)$$

C_E^0 and Γ_E^0 are the volume and surface concentrations of enzyme in the homogeneous and immobilized cases, respectively, and $[S]_{x=0}$ and $[Q]_{x=0}$ are the concentrations of substrate, S, and cosubstrate, Q, at the surface of the electrode. The bimolecular rate constants, $k_{i(\text{or } i')}$ (with $i = 1-3$) are defined as:

$$k_{i(\text{or } i')} = \frac{k_{i(\text{or } i'),1} k_{i(\text{or } i'),2}}{k_{i(\text{or } i'),1} + k_{i(\text{or } i'),2}} = \frac{k_{i(\text{or } i'),2}}{K_{i(\text{or } i'),M}} \quad (2)$$

$K_{i(\text{or } i'),M}$ being the Michaelis constant of each individual reaction i.

A more compact expression of the reaction rate, similar to that of a simple ping-pong mechanism, may be obtained by grouping together the two one-electron steps:

$$\frac{2C_E^0(\text{or } \Gamma_E^0)}{rate} = \frac{1}{k_{1,2}} + \frac{1}{k_{2,2}} + \frac{1}{k_1[S]_{x=0}} + \frac{1}{k_2[Q]_{x=0}} \quad (3)$$

with:

$$\frac{1}{k_{2,2}} = \frac{1}{k_{2',2}} + \frac{1}{k_{3',2}}$$

and

$$\frac{1}{k_2} = \frac{1}{k_{2'}} + \frac{1}{k_{3'}} \quad (4)$$

An average Michaelis constant may thus be introduced:

$$K_{2,M} = \frac{k_{2,2}}{k_2} = \frac{\frac{1}{k_{2'}} + \frac{1}{k_{3'}}}{\frac{1}{k_{2',2}} + \frac{1}{k_{3',2}}} = \frac{k_{3',2}K_{2',M} + k_{2',2}K_{3',M}}{k_{2',2} + k_{3',2}} \quad (5)$$

It has been shown with another diaphorase, a NAD(P)H quinone oxidoreductase (DT diaphorase) containing a FAD center instead of FMN, that the oxidation of the semiquinone form is faster than the oxidation of the $FADH^-$ form.[33] If this is the case with the present diaphorase too, then $k_{2,2} \simeq k_{2',2}$, $k_2 \simeq k_{2'}$, and $K_{2,M} \simeq K_{2',M}$. If not, the constants derived from the kinetic measurements would be the averaged values defined by eqs 4 and 5. It may also be envisaged that at lower pHs, the second electron transfer may involve the $FMNH^\bullet$ form (Scheme 2) concurrently with the anion radical form $FMN^{\bullet -}$. In this case, k_3 should be replaced by $k_{3'}$, defined as:

$$\frac{1}{k_3} = \frac{1 + \frac{K_3}{[H^+]}}{k_4 + \frac{K_3}{[H^+]}k_{3'}} \quad (6)$$

resulting in pH-dependent values of k_2.

Scheme 2

$$Q + E_{FMNH^\bullet} \underset{k_{4,-1}}{\overset{k_{4,1}}{\rightleftharpoons}} E_{(FMNH^\bullet,Q)} \xrightarrow{k_{4,2}} P + E_{FMNH^+} \quad [4]$$

$$E_{FMNH^+} \rightleftharpoons E_{FMN} + H^+$$

(30) (a) Xiang, B.; Markham, G. D. *Arch. Biochem. Biophys.* **1997**, *348*, 378. (b) Trimmer, E. E.; Ballou, D. P.; Matthews, R. G. *Biochemistry* **2001**, *40*, 6205. (c) Meijers, R.; Morris, R. J.; Adolph, H. W.; Merlii, A.; Lamzin, V. S.; Cedergren-Zeppezauer, E. S. *J. Chem Biol.* **2001**, *276*, 9316. (d) Pejchal, R.; Sargeant, R.; Ludwig, M. L. *Biochemistry* **2005**, *44*, 11447.

(31) (a) See refs 30b and c and references therein. (b) Anne, A.; Moiroux; J. Savéant, J.-M. *J. Am. Chem. Soc.* **1993**, *115*, 10224. (c) Bicki, J. G.; Marcinek, A.; Zielonka, J. *Acc. Chem. Res.* **2004**, *37*, 379.

(32) (a) These expressions are obtained in the same way as the equations characterizing the simple ping-pong mechanism at steady state.[26,32b] (b) Limoges, B.; Moiroux, J.; Savéant, J.-M. *J. Electroanal. Chem.* **2002**, *521*, 1.

(33) Tedeschi, G.; Chen, S.; Massey, V. *J. Biol. Chem.* **1995**, *270*, 1198.

Similar problems, which may be solved in the same way, may arise with reaction [2′] if, at lower pHs, the oxidation of the $FMNH_2$ form starts to interfere concurrently to the oxidation of the $FMNH^-$ form.

It follows that in all cases the reaction rate may be expressed (eq 3) according to the same formal kinetics as for a simple ping-pong scheme, regardless of details of the reaction mechanism, with the help of global rate constants that combine the kinetic characteristics of the elementary steps involved. The same considerations would apply for the reductive half-reaction [1], if NADH would react in a stepwise $e^- + H^+ + e^-$ or $e^- + H^\bullet$ manner rather than according to a hydride-transfer single step.

Quinones were used as two-electron acceptors, involving the associated exchange of one or two protons. If the electron and proton exchanges are concerted, the reaction is a one-step hydride-transfer process, as pictured in Scheme 1. The rate at which Q is consumed is then expressed as:

$$\frac{C_E^0(\text{or } \Gamma_E^0)}{rate} = \frac{1}{k_{1,2}} + \frac{1}{k_{2,2}} + \frac{1}{k_1[S]_{x=0}} + \frac{1}{k_2[Q]_{x=0}} \qquad (7)$$

with the same definitions of the rate constants as before. If the reaction involves stepwise $e^- + H^+ + e^-$ or $e^- + H^\bullet$ transfers, the rate expression is the same after introduction of composite rate constants combining the kinetic characteristics of the constitutive elementary steps, similarly to the case of one-electron cosubstrates we have just discussed.

The kinetic data that we have obtain in the homogeneous and immobilized cases will thus be analyzed on the basis of eq 3 or 7. It should be noted at this point that the individual values of the two first-order rate constants $k_{1,2}$ and $k_{2,2}$ cannot be derived from steady-state kinetic measurements where the substrate and cosubstrate concentrations are varied unless an additional piece of information is available. This remark leads to another formulation of eqs 3 and 7:

$$\frac{\gamma C_E^0(\text{or } \Gamma_E^0)}{rate} = \frac{1}{k_{cat}} + \frac{1}{k_1[S]_{x=0}} + \frac{1}{k_2[Q]_{x=0}} \qquad (8)$$

where:

$$\frac{1}{k_{cat}} = \frac{1}{k_{1,2}} + \frac{1}{k_{2,2}} \qquad (9)$$

and γ is a stoichiometric factor equal to 2 for one-electron cosubstrates and to 1 for two-electron cosubstrates.

Homogeneous Enzyme Kinetics. The various one-electron and two-electron cosubstrates that we used are listed in Table 1. The most complete cyclic voltammetric investigation was carried out with FcMeOH as the cosubstrate. Typical voltammograms obtained at high NADH concentrations at a screen-printed electrode (SPE, see Experimental Section) are shown in Figure 1. The voltammograms exhibit a sigmoidal shape characteristic of steady-state conditions.

At the highest cosubstrate concentration, its diffusion current starts to interfere in the catalytic response (Figure 1b), but a limiting plateau current is still reached at the upper end of the potential range. Under these conditions, the experimental plateau current, measured after subtraction of the blank response obtained in the absence of mediator and presence of NADH, is

Table 1. DI Homogeneous Rate Constants

cosubstrate	$E^{0\prime}$ (V vs SCE)[a]	k_{cat} (s^{-1})	k_2 ($M^{-1}\,s^{-1}$)[b]
$Os(bpy)_2pyCl^{2+}$	0.210	1500	8×10^8
Fc^+MeOH[c]	0.190	1600	7×10^8
PQI[d]	0.005	1300	6×10^8
ClQ[e]	−0.027	1300	1.5×10^9
2-Me-NQ[f]	−0.340	1200	1.5×10^9
2,6-AQS[g]	−0.495	250	2×10^6
2-AQS[h]	−0.540	40	6×10^5

[a] Formal potential at pH 8.5. [b] Or $k_{2\prime}$. [c] Ferrocenium methanol. [d] Parabenzoquinone imine. [e] Chloro benzoquinone. [f] 2-Methyl-naphthoquinone. [g] 2,6-Anthraquinone disulfonate. [h] 2-Anthraquinone sulfonate.

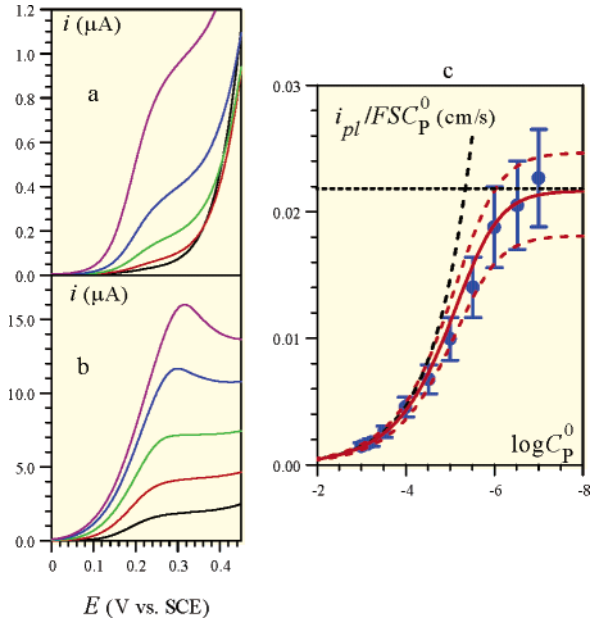

Figure 1. Linear scan voltammetry (recorded at a SPE) of DI in solution as a function of the cosubstrate (FcMeOH) concentration in a Tris buffer (pH = 8.5) containing 50 nM enzyme and 2 mM NADH. Scan rate: 10 mV/s. FcMeOH concentration: (a) from bottom to top: 0, 0.1, 0.3, 1, 3 μM; (b) from bottom to top: 10, 30, 100, 300, 1000 μM; (c) variation of the plateau current with the cosubstrate concentration. Solid circles: experimental data (standard deviation is represented by the vertical bars). The plateau currents are obtained after subtraction of a NADH blank in the absence of cosubstrate. Solid red line: best fitting with eq 12; the two dashed red lines correspond to 30% error on each rate constant. Dashed and dotted black lines: application of eqs 13 and 14, respectively.

expected to obey eq 10, after introduction of the competition parameter σ defined by eq 11.[34]

$$\frac{i_{pl}}{FSC_P^0} = 2\sqrt{\frac{k_2 C_E^0 D_P}{\gamma}}\sqrt{\frac{2}{\sigma}\left[1 - \frac{\ln(1+\sigma)}{\sigma}\right]} \qquad (10)$$

$$\sigma = k_2 C_P^0\left(\frac{1}{k_{2,2}} + \frac{1}{k_{1,2}} + \frac{1}{k_1 C_S^0}\right) \qquad (11)$$

where γ is the same stoichiometric parameter as introduced earlier, F is the faraday constant, and S is the electrode surface area. C_S^0, C_P^0, and C_E^0 are the bulk concentrations of substrate, cosubstrate, and enzyme, respectively. D_P is the cosubstrate diffusion coefficient. The cyclic voltammograms reported in Figure 1 do not change when the NADH concentration is

(34) For simplicity of notations, from here onwards, k_2 stands both for a true k_2 or for $k_{2\prime}$, as defined earlier.

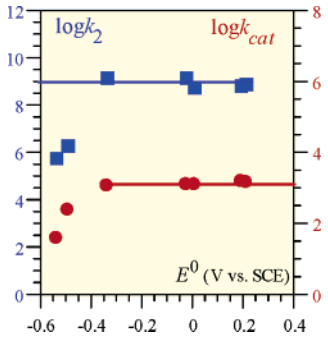

Figure 2. Variation of k_2 (M^{-1} s^{-1}) and k_{cat} (s^{-1}) with the driving force of the oxidative half-reaction.

doubled or tripled, meaning that $k_1C_S^0 \gg k_{cat}$ and, thus, that $\sigma = k_2C_P^0/k_{cat}$. Therefore:

$$\frac{i_{pl}}{FSC_P^0} = 2\sqrt{\frac{2}{\gamma}}\sqrt{\frac{k_{cat}C_E^0D_P}{C_P^0}\left[1 - \frac{\ln\left(1 + \frac{k_2C_P^0}{k_{cat}}\right)}{\frac{k_2C_P^0}{k_{cat}}}\right]} \quad (12)$$

There are two limiting behaviors for large and small values of the cosubstrate concentration, respectively:

$$\frac{i_{pl}}{FSC_P^0} = 2\sqrt{\frac{2}{\gamma}}\sqrt{\frac{k_{cat}C_E^0D_P}{C_P^0}} \quad (13)$$

$$\frac{i_{pl}}{FSC_P^0} = \sqrt{\frac{2}{\gamma}}\sqrt{k_2C_E^0D_P} \quad (14)$$

These two limits do tend to be reached at both ends of the available concentration range, as can be seen in Figure 1c. Fitting of the data points with eq 12 leads to $k_2 = (7 \pm 2) \times 10^8$ M^{-1} s^{-1} and $k_{cat} = 1600 \pm 500$ s^{-1}. Errors on the rate constants were estimated from the experimental standard deviations shown in Figure 1c and application of eq 12 with values of the rate constants 30% higher and 30% lower than the best fitting values, lead to the dashed red lines in the figure.

Similar experiments were carried out with the other one- or two-electron cosubstrates, leading to the rate constant values listed in Table 1. As the driving force offered to the oxidative half-reaction increases, k_2 tends toward a limit (Figure 2), whose value is compatible with a control by the diffusion of the cosubstrate toward the enzyme prosthetic group.[35]

Cyclic voltammetric experiments carried out at lower NADH concentrations (Figure 3) allowed the kinetic characterization of the reductive half-reaction. Decreasing NADH concentration makes the kinetic control pass progressively to reaction [1]. At the same time, diffusion of the substrate increasingly interferes, as revealed by the fact that the cyclic voltammetric responses becomes more and more peak-shaped. Simulation (see Experimental Section) of the cyclic voltammograms (Figure 3), using the values already determined for k_2 and k_{cat}, the values of the standard heterogeneous electron-transfer rate constant k_S (inferred from the fitting of CV in the absence of substrate at

(35) The value we find for this limit is ca. 10 times larger than previous literature data.[26] The reason is the unwarranted use, in the latter analysis, of the first-order approximation (eq 12) for cosubstrate concentrations that are not small enough for this approximation to be valid, as clearly appears in Figure 1c.

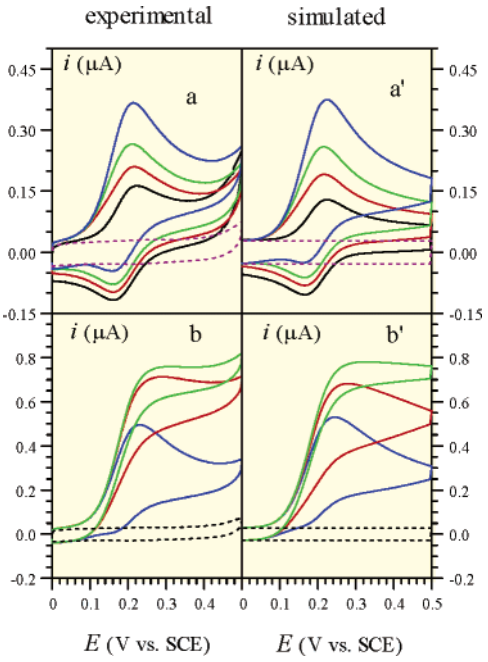

Figure 3. Cyclic voltammetry of DI in solution as a function of NADH concentration in a Tris buffer (pH = 8.5) containing 30 nM enzyme and 20 μM FcMeOH. Glassy carbon electrode. Scan rate: 10 mV/s. NADH concentration: (a) from bottom to top: 0, 10, 20, 40 μM; (b) from bottom to top: 80, 160, 320 μM. Simulations (see Experimental Section): k_s = 0.05 s^{-1}, $k_1 = 2 \times 10^7$ M^{-1} s^{-1}, $k_2 = 7 \times 10^8$ M^{-1} s^{-1}, $k_{cat} = 1600$ s^{-1}, $D_P = 6.7 \times 10^6$ cm^2 s^{-1}, $D_S = 3.5 \times 10^6$ cm^2 s^{-1}.

different scan rates), and the diffusion coefficients of the substrate, D_S, and cosubstrate, D_P, led to $k_1 = 2 \times 10^7$ M^{-1} s^{-1}. As emphasized earlier, k_{cat} is a mix of the first-order rate constants of the two half-reactions (eq 7). However, the variations of k_{cat} and k_2, with the driving force shown in Figure 2, allows for the separation of the two contributions of k_{cat}. The fact that k_2 tends toward a limit and the value of this limit clearly indicate that the oxidative half-reaction is then under diffusion control. Combining this observation with the fact that k_{cat} has also reached a limit point to the conclusion that in this range of driving force, $k_{2,2} \gg k_{1,2}$. It follows that $k_{1,2} \simeq k_{cat} = 1500$ s^{-1} leading to $K_{M,1} = 75$ μM as the value of the true Michaelis constant of the reductive half-reaction.

As seen later on, the immobilization procedures involve biotinylation of the diaphorase. Analysis of the immobilized enzyme responses thus requires determining the homogeneous kinetic characteristics of the biotinylated diaphorase (b-DI), and seeing whether biotinylation has degraded the enzyme activity. The same experiments as described above for DI were carried out with b-DI, leading to:

$$k_1 = 1.5 \times 10^7\ M^{-1}\ s^{-1}$$

$$k_2 = 3.5 \times 10^8\ M^{-1}\ s^{-1}$$

$$k_{cat} = 700\ s^{-1}$$

indicating that approximately half of the enzyme has been deactivated by the biotinylation reaction.

Immobilization. Two procedures, based on avidin−biotin affinity, were used to immobilize the enzyme on the electrode surface (Figure 4). In procedure A, a saturated monolayer of neutravidin is first adsorbed on the surface of a carbon electrode,

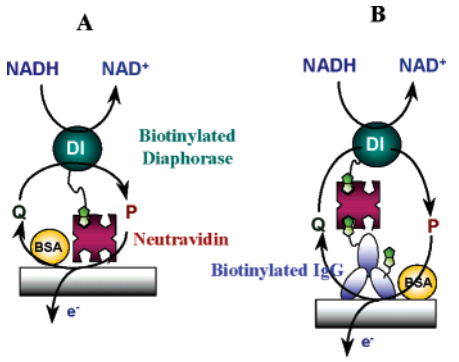

Figure 4. Two procedures for monolayer assemblage of DI on the electrode surface.

taking advantage of its hydrophobic character as a factor favoring irreversible adsorption. Bovine serum albumin (BSA) is then used to saturate the unoccupied space on the electrode surface so as to minimize nonspecific adsorption during the next step. The latter consists of soaking the electrode in a solution of biotinylated diaphorase until saturation of the avidin sites is reached. Procedure B starts with the adsorption of biotinylated rabbit immunoglobulin on the carbon surface followed by saturation with BSA and binding of neutravidin. The last step is the same as in procedure A.

In the absence of commercial sources, b-DI was prepared assuming the presence of accessible carboxylic groups on the surrounding shell of the protein that can be activated with *N*-hydroxysuccinimide before their covalent coupling to amino-derivatives of biotin. Two amine-terminated biotin reagents were tested, one having an hydrophobic alkyl linker, the *N*-(5-amino-pentyl)biotinamide, and the other an hydrophilic spacer, the biotin-poly(ethyleneglycol)-amine. Effectiveness of biotinylation was confirmed by the catalytic response obtained at a neutravidin-modified electrode incubated in a diluted solution of b-DI (0.2 μM). When a significant amount of active biotinylated enzyme was deposited on the electrode, a significant steady-state catalytic wave proportional to the enzyme coverage was recorded in the presence of FcMeOH and an excess of NADH. In contrast, a negligible catalytic response was obtained at electrodes incubated with the nonbiotinylated native DI using the same procedure. The magnitude of the steady-state catalytic currents were approximately the same for DI conjugated with the *N*-(5-amino-pentyl)biotinamide or the biotin-poly(ethyl-eneglycol)-amine. However, other attempts of biotinylation targeting external amino groups of DI or possible surrounding carbohydrate residues with sulfo-NHS-biotin or biotine hydrazide were unsuccessful. After chemical derivatization, the concentration of biotinylated DI was estimated from its FMN absorbance at 460 nm and the activity of the biotinylated DI was controlled by means of cyclic voltammetry in homogeneous solution, as detailed at the end of the previous homogeneous enzyme kinetics section.

Immobilized Enzyme Kinetics. The immobilization procedures were successful either at glassy carbon (GC) or at screen-printed electrodes (SPE, see Experimental Section). The catalytic responses are similar (Figure 5). The advantage of GC electrodes over the SPEs is that the heterogeneous electron transfer of the cosubstrate is faster, as appears in the figure. Conversely, SPEs have less residual current and are thus more suited to the investigations involving low cosubstrate concentrations, which

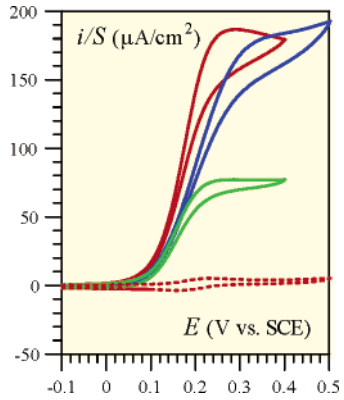

Figure 5. Cyclic voltammetry of immobilized diaphorase electrodes in a Tris buffer (pH 8.5) containing 20 μM FcMeOH and 2 mM NADH. Scan rate: 100 mV s^{-1}. Red solid line: neutravidin/b-DI-modified GC electrode, blue solid line: neutravidin/b-DI-modified SPE, green solid line: IgG-b/neutravidin/b-DI-modified GC electrode. Red dotted line: neutravidin/b-DI-modified GC electrode in the absence of NADH.

are required for the determination of large k_2 values. We also note that procedure B gives rise to responses that are about half those obtained with procedure A. For this reason, detailed kinetic analyses were restricted to electrodes derivatized according to procedure A. A first series of experiments at large NADH concentrations ($\geq$2 mM) were carried out with the same cosubstrate, FcMeOH, as in the homogeneous case. S-shaped waves, characteristic of a steady-state situation, are observed in cyclic voltammetry, as shown in Figure 5.

The plateau current may be expressed as (from ref 26 with introduction of the stoichiometric factor γ according to eq 8):

$$\frac{i}{FS} = -D_P\left(\frac{\partial[Q]}{\partial x}\right)_{x=0} + \frac{\gamma\Gamma_E^0}{\frac{1}{k_{cat}} + \frac{1}{k_1[S]_{x=0}} + \frac{1}{k_2[Q]_{x=0}}} \quad (15)$$

where the first term is the diffusion current of the cosubstrate. After subtraction of this term, the current is equal to its catalytic component:

$$\frac{i_{cat}}{FS} = \frac{\gamma\Gamma_E^0}{\frac{1}{k_{cat}} + \frac{1}{k_1[S]_{x=0}} + \frac{1}{k_2[Q]_{x=0}}} \quad (16)$$

Taking into account that at the plateau $[Q]_{x=0} = C_P^0$ and that for large excess of substrate (enzyme saturation), the plateau current is then independent of the NADH concentration in line with:

$$\frac{i_{cat,pl}}{FS} = \frac{\gamma\Gamma_E^0}{\frac{1}{k_{cat}} + \frac{1}{k_2 C_P^0}} \quad (17)$$

The results are represented in Figure 6 under the form of a reciprocal plot of the catalytic current versus the cosubstrate concentration, from the intercept and slope of which one obtains:

$$k_{cat}\Gamma_E^0 = 1.1 \times 10^{-10}\ \text{mol cm}^{-2}\ \text{s}^{-1},\ k_2\Gamma_E^0 = 0.05\ \text{cm s}^{-1}$$

We note that the ratio k_{cat}/k_2 (2.3 μM) is practically the same as in homogeneous conditions (2 μM). Since the reaction of FcMeOH with the enzyme in solution is under diffusion control,

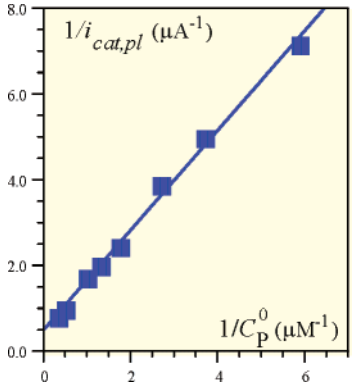

Figure 6. Plot of the reciprocal of the catalytic plateau current obtained at a neutravidin/b-DI-modified SPE as a function of reciprocal of the FcMeOH concentration. NADH concentration was in excess of 2 mM in Tris buffer (pH 8.5). Scan rate: 10 mV/s.

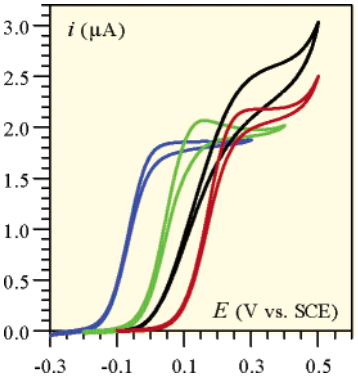

Figure 7. Cyclic voltammetry of a SPE coated with a submonolayer of neutravidin/b-DI immersed in a Tris buffer solution (pH 8.5) containing 2 mM NADH and, from left to right, $Os(bpy)_2Cl_2$, $Os(bpy)_2imCl^+$, *p*-aminophenol, and FcMeOH ($E^0 = -0.037$, 0.095, 0.005, 0.190 V vs SCE, respectively). Redox Cosubstrate: 20 μM in each case. The electrode was carefully rinsed with a buffer solution between each measurement. Scan rate: 10 mV/s.

we may assume that it is also the case with the immobilized enzyme. It follows that $\Gamma_E^0 = 0.14$ pmol cm^{-2} for the enzyme electrode used in Figure 6. By selecting the appropriate concentration of b-DI (0.1 μM) and electrode immersion time (2 h) during the immobilization of the enzyme on the neutravidin-modified electrode, the maximal enzyme surface concentration that we were able to obtain was ~1.5 pmol cm^{-2} (providing current response densities similar to those shown in Figure 5). Such an enzyme surface coverage corresponds approximately to the half-value of a theoretical closed-packed DI monolayer based on geometrical considerations.

Figure 7 shows a cyclic voltammetric experiment carried out at high substrate and cosubstrate concentrations with three additional cosubstrates (two one-electron and one two-electron exchangers) also offering a large driving force to the oxidative half-reaction, as seen in Figure 2. The limiting steady-state currents are approximately the same as with FcMeOH, thus confirming that the value of k_{cat} is independent of the nature of the cosubstrate, in line with the fact that k_{cat} is only related to the reductive half-reaction ($k_{cat} = k_{1,2}$).

The reductive half-reaction was further investigated by means of experiments where the NADH concentration is decreased to such an extent that the term $k_1[S]_{x=0}$ starts to interfere in the kinetics (see eq 16). Simultaneously, consumption of NADH in the enzyme layer ceases to be negligible, which leads to the

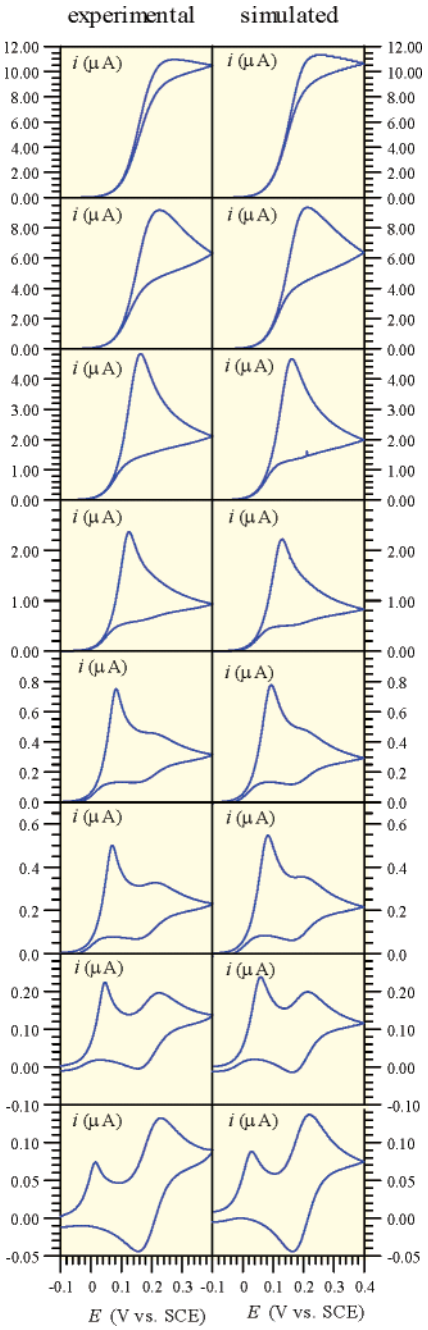

Figure 8. Cyclic voltammetry of a GC electrode coated with a monolayer of neutravidin/b-DI, immersed in Tris buffer solution, containing 20 μM of FcMeOH and increasing concentrations of NADH; from bottom to top: 10, 30, 70, 100, 300, 700, 2000, 3800 μM. Scan rate: 10 mV s^{-1}. Simulations (see Experimental Section) were performed with: $k_1 = 2 \times 10^6$ M^{-1} s^{-1}, $k_{cat} = 700$ s^{-1}, $k_2 = 3.5 \times 10^8$ M^{-1} s^{-1}, $\Gamma_E^0 = 1.5$ pM cm^{-2}, $E^0 = 0.195$ V vs. SCE, $k_S = 0.2$ cm s^{-1}, $D_S = 3.5 \times 10^{-6}$ cm^2 s^{-1}, $D_P = 6.7 \times 10^{-6}$ cm^2 s^{-1}.

progressive transformation of the plateau-shaped curves into peak-shaped curves, as shown in Figure 8, corresponding to an increasing control of the kinetics by substrate transport. Simulation of the cyclic voltammograms (see Experimental Section), knowing the values of k_{cat}, k_2, Γ_E^0, the cosubstrate formal potential, $E^{0\prime}$, the standard heterogeneous rate constant, k_S, and the substrate and cosubstrate diffusion coefficients, D_S and D_P, allows for the determination of k_1 ($k_1 = 2 \times 10^6$ M^{-1} s^{-1}). We note that this value is significantly lower than the value found for the biotinylated enzyme in solution ($k_1 = 1.5 \times 10^7$ M^{-1}

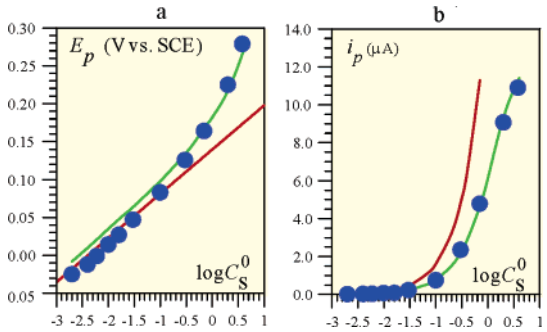

Figure 9. Variation of the peak potential (a) and peak current (b) with the substrate concentration (mM) for the same conditions as in Figure 8. Green lines: simulation. Red lines: application of eq 19 (a) and (18) (b).

s^{-1}), in contrast with the unchanged values of $k_{1,2}$ and k_2. This decreased reactivity may be caused by a steric disturbance of the recognition of NADH by the enzyme,[36] owing to random orientation of the enzyme on the electrode surface.

As the substrate concentration decreases, the peak sharpens and shifts in the negative direction until the current is entirely controlled by substrate diffusion, while the location of the peak still depends on the enzyme kinetics, as summarized by eqs 18 and 19 for a nernstian redox mediator.[26,37]

$$i_p = 2FSC_S^0\sqrt{D_S}\sqrt{\frac{Fv}{RT}} \tag{18}$$

$$E_p = E^0 - \frac{RT}{F}\ln\left(\frac{\Gamma_E^0 k_2 C_P^0}{C_S^0\sqrt{D_S}\sqrt{\frac{Fv}{RT}}}\right) \tag{19}$$

Figure 9a shows the variation of the peak potential with the cosubstrate concentration and illustrates the reaching of the limiting behavior characterized by eq 18 for very low concentrations. It is remarkable that, while the peak current no longer contains kinetic information about the enzymatic reaction, the peak potential does, its determination providing another access to k_2. The variation of the peak (or plateau current), shown in Figure 9b, provides a calibration curve for the determination of NADH. Two features of this curve are worth noting. One is that the spread of accessible concentrations is quite wide (from an estimated detection limit of 0.2[38] to 10 000 μM). The other concerns the lower end of the concentration range, where the peak current becomes proportional to NADH concentration (eqs 18). Catalysis is then maximal (total catalysis), producing a current that is equal to the current for the direct oxidation of the substrate at a much less demanding potential. This result, obtained with a monolayer enzyme coating, supports the idea that thick coatings are not required to obtain a maximal catalytic efficiency for low substrate concentrations. It may even be not only useless but also counterproductive to increase thickness because transport through a thicker film may become a limiting factor.

Another important point in terms of analytical applications of diaphorase concerns its potential use as a sensitive electrochemical enzyme label to indirectly sense the specific biomolecular recognition occurring at a bioaffinity electrode (e.g., immuno- or DNA-electrode). The degree of analytical performance (sensitivity and detection limit) of the bioaffinity electrode is related to the capacity to detect electrochemically low surface concentration of the enzyme label specifically anchored on the electrode surface. This can be estimated from following equations obtained at saturation of the substrate Michaelis−Menten kinetics:

$$\Gamma_E^0 = \frac{i_{cat,pl}/S}{2Fk_{cat}} \tag{20}$$

Taking, as earlier, 45 nA/cm^2 as the lowest detectable current density,[38] the biotinylated diaphorase electrode (turnover k_{cat} of 700 s^{-1}), operating with ferrocenemethanol as cosubstrate and NADH as substrate, is expected to allow a detection limit of 4×10^{-16} M cm^{-2}, a value that compares favorably with those obtained by the application of advanced fluorescence techniques.[39] According to eq 20, the key parameter for the low detection limit of an enzyme label is its turnover number, k_{cat}. The higher the turnover, the lower the detection limit. The values of 1500 s^{-1} for DI or 700 s^{-1} for b-DI are higher than the turnover measured for the horseradish peroxidase ($k_{cat} = 280$ s^{-1}) in the presence of the $[Os(bpy)_2pyCl]^{2+/+}$ mediator and its H_2O_2 substrate.[24] The diaphorase should thus replace advantageously the horseradish peroxidase label commonly used in the bioelectrocatalytic detection of DNA on an electrode surface or in immunoelectrochemical sensing applications.[40] The turnover of DI is also competitive with those of glucose oxidase ($k_{cat} = 600$ s^{-1}),[23] an enzyme label which has been recently used for amperometric detection of nucleic acid at femtomolar level.[41]

Concluding Remarks

Two immobilization procedures based on the affinity of biotinylated diaphorase (from *Bacillus stearothermophilus*) for a monolayer of neutravidin adsorbed on the electrode directly or by means of a monolayer of biotinylated rabbit immunoglobulin appear to be mild enough not to damage the catalytic activity of the enzyme. The activity of the native diaphorase is decreased by the biotinylation reaction to about one-half, but the immobilization procedures themselves are harmless. This conclusion could only be arrived at after a careful and systematic kinetic analysis of the electrochemical responses of the immobilized enzyme in the presence of variable concentrations of substrate and cosubstrate, leading to an estimation of the active enzyme coverage. This required a thorough quantitative reexamination of the kinetics of the enzyme in solution to be compared with its immobilized counterpart. Sensitivity of the electrochemical current responses to the NADH concentration cover a remarkably large range expanding over more than 4 orders of magnitude. It is also worth noting that at the lower

(36) The specific recognition of NADH by DI was confirmed from a total absence of catalysis in homogeneous solution when NADH is replaced by NADPH.
(37) For a reversible electron transfer between the cosubstrate and the electrode, which is closely the case for the low currents thus observed (Figure 9).
(38) Considering a background noise of 15 nA cm^{-2} at 10 mV s^{-1} and a signal-to-noise ratio of 3.
(39) Lehr, H.-P.; Reimann, M.; Brandenburg, A.; Sulz, G.; Klapproth, H. *Anal. Chem.* **2003**, *75*, 2414. The detection limit of the Cy5 fluorescent probe by total internal reflection fluorescence applied to DNA microarray was estimated to be of ~2 molecules/μm^2, i.e., $\Gamma \approx 3 \times 10^{-16}$ mol cm^{-2}.
(40) (a) de Lumley-Woodyear, T.; Caruana, D. J.; Campbell, C. N.; Heller, A. *Anal. Chem.* **1999**, *71*, 394. (b) Zhang, Y.; Kim, H.-H.; Heller, A. *Anal. Chem.* **2003**, *75*, 3267. (c) Zhang, Y.; Heller, A. *Anal. Chem.* **2005**, *77*, 7758. (d) Campbell, C. N.; Lumley-Woodyear, T.; Heller, A. *Fresenius' J. Anal. Chem.* **1999**, *364*, 165.
(41) Xie, H.; Zhang, C.; Gao, Z. *Anal. Chem.* **2004**, *76*, 1611.

end of the concentration range, a single monolayer is sufficient to produce the maximal catalytic response, which emphasizes the idea that a thick coating of DI may not only be unnecessary but also counterproductive. Concerning the practical application of the diaphorase electrode for NADH analysis in biological samples, the results obtained with different redox mediators show that by selecting an appropriate mediator with a formal potential in the region −0.3 to 0.0 V vs SCE, it is possible to eliminate most of the undesirable interferences of easily oxidizable species, such as ascorbate, urate, and acetaminophen (these compounds are oxidized at potentials ≫ 0 V SCE[42]), without affecting the analytical performance (the kinetics rate constants k_2 and k_{cat} of DI were approximately the same whatever the mediator). Finally, the data that we have gathered as a result of a quantitative analysis of the cyclic voltammetric responses indicate that amounts of enzyme as low as a few tenths of a femtomole per square centimeter should be detectable. These numbers compare favorably with the levels that can be reached by advanced fluorescence techniques and even with the most efficient redox enzyme labels currently used in electrochemical enzyme affinity assays. They are also promising for the design and optimization of pluri-enzymatic systems in current development, which aim at further boosting the catalytic responses by the association of other enzymes with immobilized diaphorase.

Experimental Section

Reagents. NADH (Sigma), *p*-aminophenol (PAP) (Prolabo), bovine serum albumin (BSA) (Sigma), *N*-hydroxysuccinimide (NHS) (Aldrich), 1-ethyl-3-[3-dimethylaminopropyl]carbodiimide hydrochloride (Uptima), *N*-(5-aminopentyl)biotinamide trifluoroacetate salt (Sigma), chrompure biotinylated rabbit IgG (Pierce), and neutravidin (Pierce) were used as received. Ferrocenyl methanol (Aldrich) was recrystallized twice from toluene and cyclohexane. $[Os(bpy)_2pyCl]PF_6$ and $[Os(bpy)_2$-$imCl]PF_6$ were synthesized as previously described.[43] 2-AQS, 2,6-AQS, 2-Me-NQ, and ClQ (Aldrich) were used as received. Lyophilised Diaphorase from *Bacillus stearothermophilus* (E.C. 1.6.99.-) was purchased from Unitika (Japan). The phosphate buffer saline (PBS) of pH 7.4 was prepared from 4.3 mM NaH_2PO_4, 15.1 mM Na_2HPO_4, and 50 mM NaCl. The 0.1 M Tris buffer of pH 8.5 was prepared from 4.42 g L^{-1} Trizma base (Sigma) and 8.72 g L^{-1} Trizma, HCl (Sigma). All aqueous solutions were prepared with water purified by a Milli-Q water purification system from Millipore.

Biotinylation of Diaphorase. A mixture of 0.5 mL of NHS (2 mg) and EDC (0.7 mg) in MES was reacted during 15 min with 0.93 mg of lyophilized diaphorase dissolved into 0.5 mL of 0.1 M 2-[*N*-morpholino]-ethane sulfonate buffer (MES, pH 5.5). After the addition of 0.5 mL of *N*-(5-amino-pentyl)biotinamide (2.7 mg) in MES, the mixture was left at room temperature for 3 h and then was passed through a dextran desalting column (Pierce) to remove the excess of reagents. The collected enzymatic solution (∼2.5 mL) was next centrifuged (14000g for 10 min) using a microconcentrator (10 000 MW cutoff, Nanosep, Pall) and washed four times with PBS. The concentrated biotinylated DI was finally recovered in 1 mL of PBS, and its concentration was determined spectrophotometrically using a FMN extinction coefficient of 12 000 M^{-1} cm^{-1} at 460 nm.[6]

Immobilization of Biotinylated Diaphorase on Carbon Electrodes. All experiments were performed at room temperature. A drop of 8 μL of 5 mg mL^{-1} biotinylated rabbit IgG in PBS was locally deposited on the sensing area of the carbon electrode (GC or SPE) and incubated for 2 h in a water-saturated atmosphere. The electrode surface was next thoroughly rinsed with PBS and immersed overnight in a solution of 10 μg mL^{-1} neutravidin prepared in PBS and containing 0.1% BSA. After another thorough washing with PBS, the biotinylated enzyme was immobilized by dipping the electrode for at least 2 h in a 0.1 μmol L^{-1} biotinylated diaphorase diluted in PBS. For control experiments, the first layer of biotinylated IgG was replaced by BSA. Electrodes directly coated with neutravidin were prepared by deposition of a 8 μL drop of a 1 mg mL^{-1} neutravidin on the electrode surface for 2 h under a water-saturated atmosphere. After rinsing with PBS, the modified electrodes were immersed for 15 min in a 0.1% BSA solution in PBS and next were incubated for at least 2 h in 0.1 μmol L^{-1} biotinylated diaphorase in PBS. Once prepared, the enzyme electrodes were stored in PBS at 4 °C until used.

Electrochemical Experiments. Cyclic voltammetry and chronoamperometry measurements were performed with an AUTOLAB potentiostat, PGSTAT 12 (Ecochemie), interfaced to a PC computer (GPES software). The experiments were performed in a water-jacketed electrochemical cell maintained at 20 ± 0.5 °C with a circulating water bath. All measurements were carried out at 20 °C in a 0.1 M Tris buffer solution (pH 8.5), using a saturated calomel electrode (SCE) as a reference electrode and a platinum wire as a counter electrode. Working electrodes were either glassy carbon electrodes (3-mm diameter) or screen-printed electrodes (3.5-mm diameter) prepared from a homemade graphite/polystyrene ink as previously described.[44] In the case of homogeneous DI kinetics, the working electrode was saturated with a monolayer of BSA by immersion for 30 min in a PBS buffer containing 0.1% BSA. The pretreatment of the electrode by a hydrophilic layer of BSA allowed us to improve the reproducibility of the CV measurements.

Quantitative Analysis of the Plateau Currents and Digital Simulation. The diffusion coefficients of the cosubstrates were obtained from the cyclic voltammetric oxidation peak currents at different concentrations and scan rates: $D_{FcMeOH} = 6.7 \times 10^{-6}$ cm^2 s^{-1}, $D_{PAP} = 3 \times 10^{-6}$ cm^2 s^{-1}, $D_{Os(bpy)2pyCl} = 5 \times 10^{-6}$ cm^2 s^{-1}, $D_{ClQ} = 3.5 \times 10^{-6}$ cm^2 s^{-1}, $D_{2\text{-}AQS} = 4 \times 10^{-6}$ cm^2 s^{-1}, $D_{2\text{-}Me\text{-}NQ} = 5.7 \times 10^{-6}$ cm^2 s^{-1}, $D_{2,6\text{-}AQS} = 4.5 \times 10^{-6}$ cm^2 s^{-1}. The diffusion coefficient of NADH was taken from ref 45 ($D_{NADH} = 3.5 \times 10^{-6}$ cm^2 s^{-1}).

Simulations of cyclic voltammograms for homogeneous catalysis were carried out with the DigiElch software of M. Rudolph (http://www.digielch.de/).[46] The enzyme in homogeneous solution was considered as practically immobile as compared with the cosubstrate (enzyme diffusion coefficient of 10^{-10} cm^2 s^{-1}).

A homemade digital simulator software,[47] based on a similar calculation technique as previously published,[24,26] was used to simulate the cyclic voltammograms obtained with the immobilized-diaphorase electrodes.

JA0569196

(42) (a) Wang, J.; Wu, H. *J. Electroanal. Chem.* **1995**, *395*, 287. (b) Wang, J.; Liu, J.; Chen, L.; Lu, F. *Anal. Chem.* **1994**, *66*, 3600.
(43) Kober, E. M.; Caspar, J. V.; Sullivan, B. P.; Meyer, T. J. *Inorg. Chem.* **1988**, *27*, 4587.
(44) Bagel, O.; Limoges, B.; Schöllhorn, B.; Degrand, C. *Anal.Chem.* **1997**, *69*, 4688.
(45) Samec, Z.; Elving, P. J. *J. Electroanal. Chem.* **1983**, *144*, 217.
(46) Rudolph, M. *J. Electroanal. Chem.* **2003**, *543*, 23.
(47) In preparation.